Electrical Properties of PCCYA-doped ZnO-based Varistors

Choon-Woo Nahm[a]
Department of Electrical Engineering, Dongeui University,
995 Eomgwangno, Busanjin-gu, Busan 614-714, Korea

[a]E-mail : cwnahm@deu.ac.kr

(Received March 17 2008, Accepted June 10 2008)

The microstructure, voltage-current, and capacitance-voltage relations of PCCYA doped ZnO-based varistors were investigated for different amounts of Al_2O_3. As the Al_2O_3 amount increased, the average grain size (d) increased from d=4.3 to d=5.5 μm and the sintered density (ρ) increased from ρ=5.63 to ρ=5.67 g/cm^3. As the Al_2O_3 amount increased, the breakdown voltage (V_B) increased from V_B=633 to V_B=71 V/mm and the non-ohmic coefficient (α) increased from α=47 to α=4. Al_2O_3 served as a donor due to the donor density (N_d), which increases in the range of N_d=0.77-1.85×10^{18}/cm^3 with increasing amount of Al_2O_3.

Keywords : Microstructure, Al_2O_3, Electrical properties, Varistors

1. INTRODUCTION

Pure zinc oxide exhibits ohmic properties even at any sintering condition, whereas the zinc oxide doped with several different metal oxides exhibits non-ohmic properties, which give rise to the decrease of impedance with increasing voltage. This non-ohmicity of current-voltage properties is due to the presence of a double Schottky barrier (DSB) formed at the active grain boundaries containing many trap states. Owing to highly nonlinear properties, ZnO varistors are used widely in the field of overvoltage protection systems from electronic circuits to electric power systems[1,2]. ZnO varistors are generally divided into two categories, called Bi_2O_3-based and Pr_6O_{11}-based ceramics, in terms of varistor forming oxides. ZnO-Bi_2O_3-based ceramics have been mainly studied in different aspects since discovery of ZnO non-ohmic ceramics. Although ZnO-Bi_2O_3-based ceramics show excellent non-ohmic properties, Bi_2O_3 easily reacts with some metals used in preparing multilayer chip non-ohmic ceramics, and it destroys the multilayer structure[3]. And it is reported to have an additional insulating spinel phase, which does not play any role in electrical conduction[3]. Recently, ZnO-Pr_6O_{11}-based ceramics have been studied in order to improve a few drawbacks[3] associated with Bi_2O_3 [4-11].

To solve these problems and to obtain the high performance, it is very important to comprehend the additives-doping effect on non-ohmic properties. Al_2O_3 is often added to ZnO-Bi_2O_3-based varistors to improve the performance[12-14]. However, the role of Al_2O_3 in the ZnO-Pr_6O_{11}-based varistors was found to partially differ from the ZnO-Bi_2O_3-based varistors in a few respects.

In this work, Al_2O_3 doping effect on microstructure and electrical properties of Pr-Co-Cr-Y-doped ZnO-based varistors were investigated.

2. EXPEIMENTAL PROCEDURE

2.1 Sample preparation

Reagent-grade raw materials were used for preparing the varistors with a composition of (97.5-x) mol% ZnO, 0.5 mol% Pr_6O_{11}, 1.0 mol% CoO, 0.5 mol% Cr_2O_3, 0.5 mol% Y_2O_3, x mol% Al_2O_3 (x = 0.001, 0.005, 0.01, 0.1). Raw materials were mixed by ball milling with zirconia balls and acetone in a polypropylene bottle for 24 h. The mixture was dried at 120 °C for 12 h and calcined in air at 750 °C for 2 h. The calcined mixture was pulverized using an agate mortar/pestle and after 2 wt% polyvinyl alcohol (PVA) binder addition, granulated by sieving 100-mesh screen to produce starting powder. The powder was uniaxially pressed into discs of 10 mm in diameter and 2 mm in thickness at a pressure of 800 kg/cm^2. The discs were covered with raw powder in alumina crucible, sintered at 1280 °C for 1 h. The sintered samples were lapped and polished to 1.0 mm thickness. The final samples were about 8 mm in diameter and 1.0 mm in thickness. Silver paste was coated on both faces of the samples and ohmic contact of electrodes was formed by heating at 600 °C for 10 min. The electrodes were 5 mm in diameter.

2.2 Microstructure examination

Both sides of the samples was lapped and ground with SiC paper and polished with Al_2O_3 powders to a mirror-like surface. The polished samples were thermally etched at 1100 °C for 30 min. The surface microstructure was examined by a scanning electron microscope (SEM, Hitachi S2400, Japan). The average grain size (d) was determined by the lineal intercept method as follows:

$$d = \frac{1.56L}{MN} \tag{1}$$

where L is the random line length on the micrograph, M is the magnification of the micrograph, and N is the number of the grain boundaries intercepted by lines[15]. The crystalline phases were identified by an X-ray diffractometry (XRD, Rigaku D/max 2100, Japan) with CuK_α radiation. The sintered density (ρ) of ceramics was measured by the Archimedes method.

2.3 Electrical measurement

The V-I characteristics of the varistors were measured using a high voltage source measure unit (Keithley 237). The breakdown voltage (V_B) was measured at a current density of 1.0 mA/cm^2 and the leakage current (I_L) was measured at 0.80 V_B. In addition, the nonlinear coefficient (α) was determined from the following expression.

$$\alpha = \frac{\log J_2 - \log J_1}{\log E_2 - \log E_1} \tag{2}$$

where J_1 = 1.0 mA/cm^2, J_2 = 10 mA/cm^2, and E_1 and E_2 are the electric fields corresponding to J_1 and J_2, respectively.

The capacitance-voltage (C-V) characteristics of varistors were measured at 1 kHz using a RLC meter (QuadTech 7600) and an electrometer (Keithley 617). The donor concentration (N_d) and the barrier height (ϕ_b) were determined by the equation $(1/C_b\text{-}1/C_{bo})^2 = 2(\phi_b+V_{gb})/q\varepsilon N_d$[16], where C_b is the capacitance per unit area of a grain boundary, C_{bo} is the value of C_b when $V_{gb}=0$, V_{gb} is the applied voltage per grain boundary, q is the electronic charge, and ε is the permittivity of ZnO ($\varepsilon=8.5\varepsilon_o$). The density of interface states (N_t) at the grain boundary was determined by the equation $N_t=(2\varepsilon N_d\phi_b/q)^{1/2}$[16].

3. RESULTS AND DISCUUSION

Figure 1 shows the SEM micrographs of the samples for different amounts of Al_2O_3. The samples added with Al_2O_3 exhibited the same phases composition as the sample without Al_2O_3[4]. For all the samples, the XRD patterns, as shown in Fig. 2, revealed the presence of Pr-

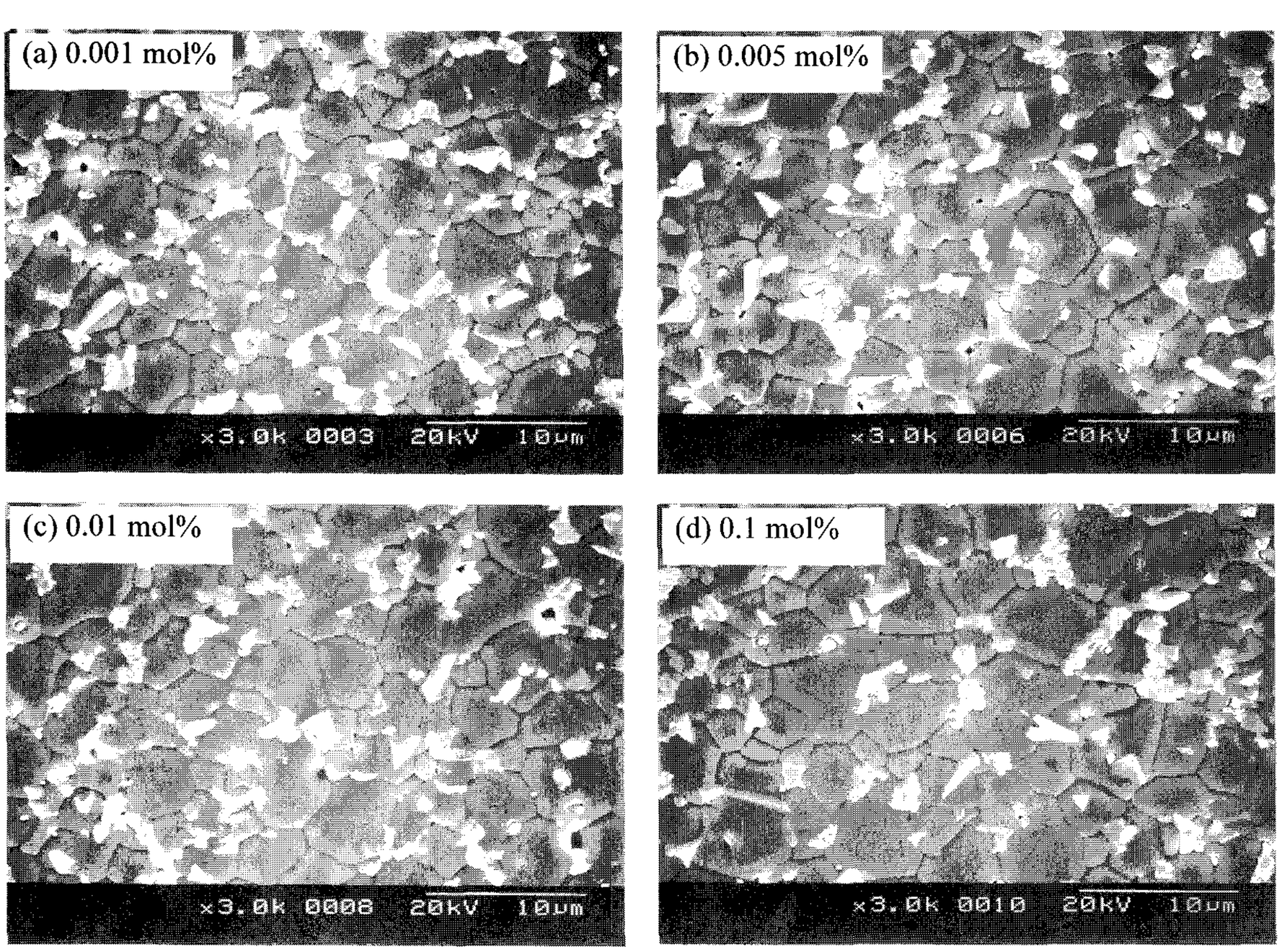

Fig. 1. SEM micrographs of the samples for different amounts of Al_2O_3.

and Y-rich intergranular layer (whitish) as a minor secondary phase, in addition to a major phase of hexagonal ZnO (blackish). No $ZnAl_2O_4$ spinel phase related to Al was detected. Therefore, it is assumed that the majority of Al atoms are solved into ZnO matrix, because Al^{3+} ionic radius is smaller than that of Zn^{2+}. The average grain size (d) increased from 4.3 to 5.5 μm with the increase of amount of Al_2O_3. As a result, Al_2O_3 acted as a prompter for grain growth. If spinel phase of $ZnAl_2O_4$ was formed, the grain average size would be reduced due to the inhibition of ZnO grain growth. The sintered density (ρ) slightly increased from 5.63 to 5.67 g/cm^3 corresponding to 97.4-98.1 % of theoretical density (TD=5.78 g/cm^3 in ZnO). Al_2O_3 doping did not significantly modify the densification process. However, it should be noted that the behavior of the grain size and sintered density with the increase of amount of Al_2O_3 showed the opposite results compared with Bi_2O_3-based ZnO samples[12-14]. The detailed microstructure parameters are summarized in Table 1.

Figure 3 shows the E-J characteristics of the samples for different amounts of Al_2O_3. The curves show the conduction characteristics divided into two regions: an ohmic region before the breakdown field and a non-ohmic region after the breakdown field. The sharper the knee of the curves between the two regions, the better the nonlinear properties. On adding more Al_2O_3, the knee gradually becomes less pronounced and as a result, the non-ohmic properties are deteriorated. Therefore, an appropriate addition of Al_2O_3 seems to enhance non-ohmic properties, whereas an excess addition results in bad non-ohmic properties.

The breakdown voltage (V_B) greatly decreased from V_B=633 to V_B=71 V/mm with the increase of amount of Al_2O_3. This is attributed firstly to the decrease of the number of the grain boundaries caused by the increase of the ZnO grain size, and secondly, to the decrease of breakdown voltage per grain boundary (v_{gb}). The v_{gb} is calculated by the following equation: $V_B = N_{gb} \cdot v_{gb} = (D/d)\, v_{gb}$, where V_B is the breakdown voltage, N_{gb} is the number of the grain boundaries, d is the average grain size, and D is the thickness of sample. The samples added with Al_2O_3 more than 0.1 mol% exhibited much lower v_{gb} (0.4 V/gb) value than a general value of 2-3 V/gb. These samples will exhibit very poor non-ohmic properties presumably. It should be noted that the behavior of E_B showed the different result in comparison to ZnO-Bi_2O_3-based samples[13,14].

The non-ohmic coefficient (α) slightly increased from α=44 to α=47 with increasing amount of Al_2O_3 at less

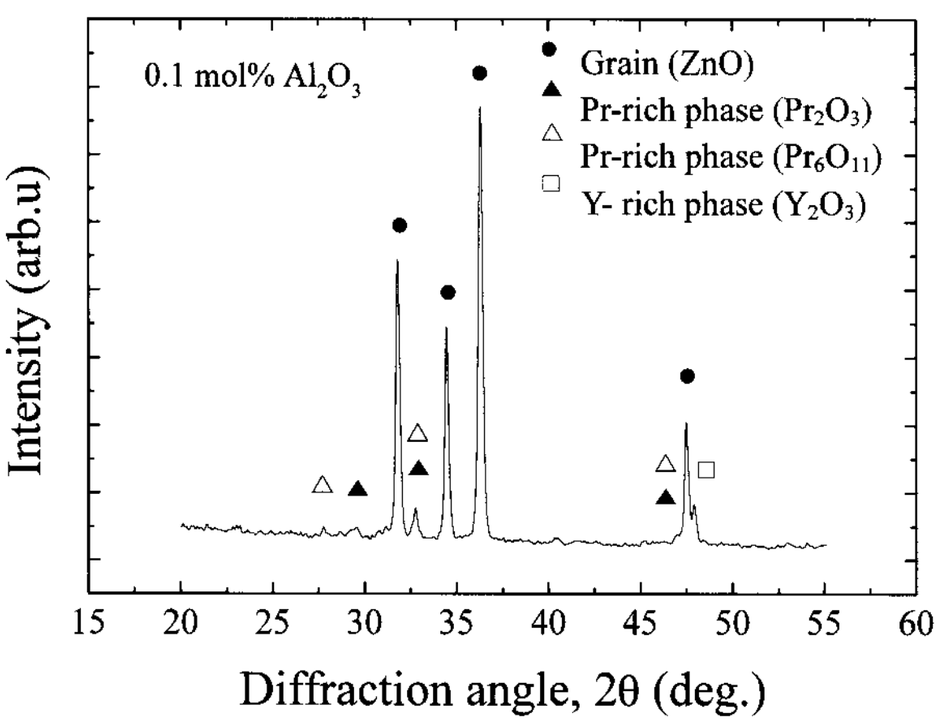

Fig. 2. XRD patterns of the samples.

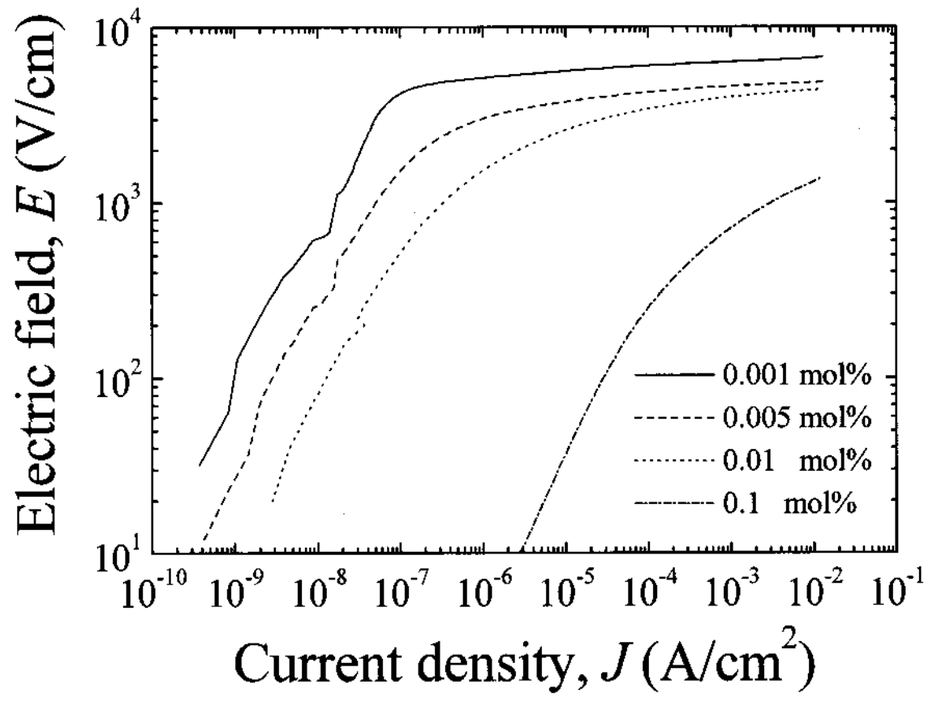

Fig. 3. E-J characteristics of the samples for different amounts of Al_2O_3.

Table 1. Microstructure, V-I, and C-V characteristic parameters of the samples for different amounts of Al_2O_3.

Al_2O_3 amount (mol%)	d (μm)	ρ (g/cm^3)	V_B (V/cm)	v_{gb} (V/gb)	α	I_L (μA)	N_d ($10^{18}cm^{-3}$)	N_t ($10^{12}cm^{-2}$)	Φ_b (eV)
0.001	4.3	5.63	633	2.7	44	0.1	0.77	3.12	1.35
0.005	4.8	5.65	461	2.2	47	1.4	1.51	4.45	1.40
0.01	5.2	5.66	401	2.1	25	9.7	1.85	4.61	1.22
0.1	5.5	5.67	71	0.4	4	0.1 mA	-	-	-

than 0.005 mol%. However, the further additions greatly decreased it and only α=4 at 0.1 mol%. Although only 0.1 mol% in Al_2O_3 amount compared with general adders is never a lot of amounts, it deteriorated non-ohmic properties. The leakage current (I_L) increased from I_L=0.1 μA to I_L=0.1 mA with increasing amount of Al_2O_3. As a result, it was confirmed that Al_2O_3 has a strong effect on the non-ohmic properties. It is assumed that Al_2O_3 doping effect on non-ohmic properties is related to electronic state at the grain boundary. The detailed V-I characteristic parameters are summarized in Table 1.

Figure 4 shows the C-V characteristics of the samples for different amounts of Al_2O_3. It is assumed that the C-V characteristics for different amounts of Al_2O_3 will vary because the C-V characteristic curves are variously arranged according to different amounts of Al_2O_3. The C-V parameters such as the donor density (N_d), barrier height (Φ_b), and density of interface states (N_t) are summarized in Table 1. The increase of Al_2O_3 amount resulted in the increase of the donor density (N_d) from $N_d=0.77\times10^{18}/cm^3$ to $N_d=1.85\times10^{18}/cm^3$. It is believed that positively charged trivalent Al ion easily substitutes for the positively charged divalent Zn ion site, because trivalent Al ionic radius is smaller than that of divalent Zn ion. The chemical-defect reaction using Kroger-Vink notation can be written as the following equation: $Al_2O_3 \xrightarrow{ZnO} Al_{Zn}^{\cdot} + e' + 3O_O^{\times}$, where $Al_{Zn}^{\cdot}$ is a positively charged Al ion substituted for Zn lattice site and $O_O^{\times}$ is a neutral oxygen of oxygen lattice site. The electron generated in reaction above increases the donor concentration. So, Al_2O_3 increases electron carrier density by exciting electron to conduction band. As a result, the positively charged trivalent Al ion served as a donor, as previously reported data[12]. The density of interface states (N_t) increased from $N_t=3.12\times10^{12}/cm^2$ to $N_t=4.61\times10^{12}/cm^2$ with the increase of amount of Al_2O_3.

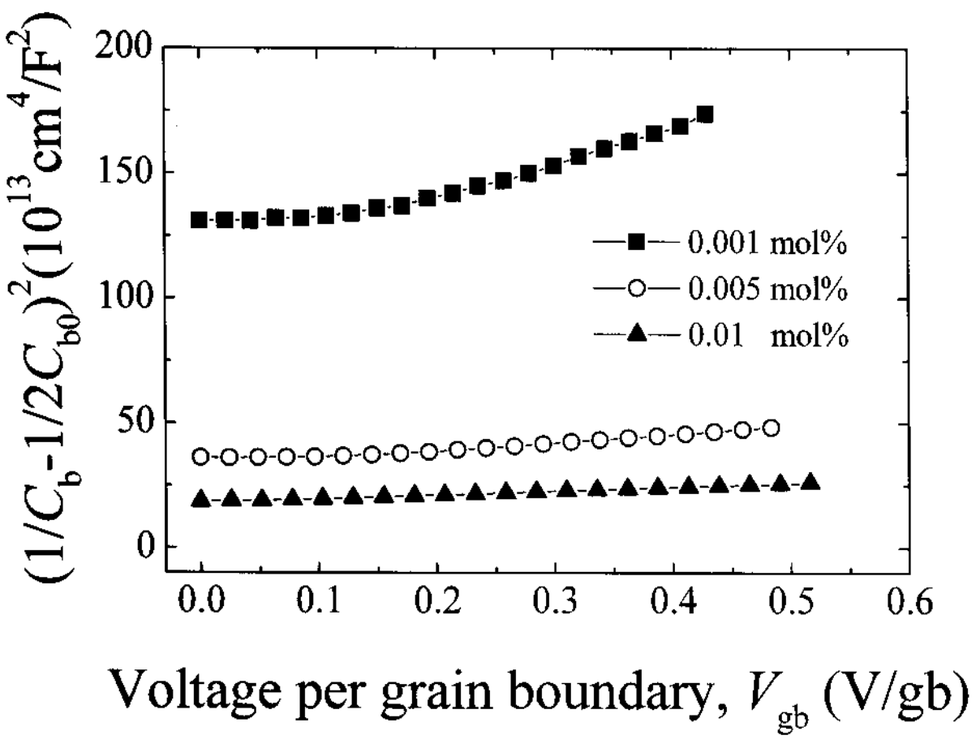

Fig. 4. C-V characteristics of the samples for different amounts of Al_2O_3.

For the amount of Al_2O_3 less than 0.005 mol%, the barrier height (Φ_b) at the grain boundaries increased up to maximum value (1.40 eV) at 0.005 mol%. The further additions decreased it and it exhibited a minimum value (1.22 eV) at 0.01 mol% (not measured for 0.1 mol%). This coincides with the variation of the α in E-J characteristics.

4. CONCLUSION

The microstructure and electrical properties of varistors PCCYA-doped ZnO-based varistors were investigated for different amount of Al_2O_3. The average grain size (d) slightly increased from d=4.3 to d=5.5 μm with increasing amount of Al_2O_3. As the Al_2O_3 amount increased, the breakdown voltage increased from V_B=633 to V_B=71 V/mm and the non-ohmic coefficient increased from α=47 to α=4. Al_2O_3 served as a donor Al_2O_3 served as a donor due to the donor density (N_d), which increases in the range of $N_d=0.77\text{-}1.85\times10^{18}/cm^3$ with increasing amount of Al_2O_3.

ACKNOWLEDGEMENT

This work was supported by Dongeui University grant (No. 2007AA174).

REFERENCE

[1] L. M. Levinson and H. R. Philipp, "Zinc oxide varistor-a review", Amer. Ceram. Soc. Bull., Vol. 65, No. 4, p. 639, 1986.
[2] T. K. Gupta, "Application of zinc oxide varistor", J. Amer. Ceram. Soc., Vol. 73, No. 7, p. 1817, 1990.
[3] Y. S. Lee and T. Y. Tseng, "Phase identification and electrical properties in ZnO-glass varistors", J. Amer. Ceram. Soc., Vol. 75, No. 6, p. 1636, 1992.
[4] C.-W. Nahm, "Microstructure and electrical properties of Y_2O_3 doped ZnO-Pr_6O_{11}-based varistor", Mater. Lett., Vol. 57, No. 7, p. 1317, 2003.
[5] C.-W. Nahm and B.-C. Shin, "Highly stable electrical properties of ZnO-Pr_6O_{11}-CoO-Cr_2O_3-Y_2O_3-based varistor cearmics", Mater. Lett., Vol. 57, No. 7, p. 1322, 2003.
[6] C.-W. Nahm, "Microstructure and electrical properties of Dy_2O_3-based ZnO-Pr_6O_{11}-based varistor ceramics", Mater. Lett., Vol. 58, No. 17-18, p. 2252, 2004.
[7] C.-W. Nahm and B.-C. Shin, "Effect of sintering time on electrical characteristics and DC accelerated aging behaviors of Zn-Pr-Co-Cr-Dy oxide-based

varistors", J. Mater. Sci.: Mater. Electron., Vol. 16, No. 11-12, p. 725, 2005.
[8] C.-W. Nahm, "Effect of sintering temperature on microstructure and electrical properties of Zn·Pr·Co·Cr·La oxide-based varistors", Mater. Lett., Vol. 60, No. 28, p. 3394, 2006.
[9] C.-W. Nahm, " Effect of La_2O_3 addition on electrical characteristics of Pr_6O_{11}-based ZnO varistors", Trans. EEM, Vol. 7, No. 3, p. 123, 2006.
[10] C.-W. Nahm, "Electrical properties of ZPCCT-based varistor ceramics", Trans. EEM, Vol. 8, No. 3, p. 105, 2007.
[11] C.-W. Nahm, "Electrical properties and stability of Tb-doped ZnO-based nonlinear resistors", Solid State Commun., Vol. 141, No. 12, p. 685, 2007.
[12] S. I. Nunes and R. C. Bradt, "Grain growth of ZnO in $ZnO-Bi_2O_3$ ceramics with Al_2O_3 additions", J. Am. Ceram. Soc., Vol. 78, p. 2469, 1995.
[13] M.-H. Wang, K.-A. Hu, B.-Y. Ahao, and N.-F. Ahang, "Electrical characteristics and stability of low voltage ZnO varistors doped with Al", Mater. Chem. Phys., Vol. 100, p. 142, 2006.
[14] S. Bernik and N. Daneu, "Characteristics of ZnO-based varistor ceramics doped with Al_2O_3", J. Europ. Ceram. Soc., Vol. 27, p. 3161, 2007.
[15] J. C. Wurst and J. A. Nelson, "Lineal intercept technique for measuring grain size in two-phase polycrystalline ceramics", J. Amer. Ceram. Soc., Vol. 55, No. 97-12, p. 109, 1972.
[16] M. Mukae, K. Tsuda, and I. Nagasawa, "Capacitance-vs-voltage characteristics of ZnO varistor", J. Appl. Phys., Vol. 50, No. 6, p. 4475, 1979.